RESEARCH ARTICLE

Design and Evaluation of Solid Lipid Nanoparticle Eye Drops Containing VRN for Ocular Drug Delivery

Raffah K. Mahal*, Fatima Al-Gawhari

College of pharmacy, University of Baghdad, Iraq

Received: 10th October, 2022; Revised: 22nd November, 2022; Accepted: 02nd December, 2022; Available Online: 25th December, 2022

ABSTRACT

As a well-known oral and intravenous antifungal, voriconazole (VRN) has an extensive history of usage in the medical field. Solid lipid nanoparticles (SLNs) have been produced to treat ocular fungal keratitis in the eye. A 3^2Box-behnken design was used to produce a variety of new formulas for hot-melt extrusion. The SLNs were evaluated by entrapment efficiency (EE percent), particle size (PS), polydispersity index (PDI), and zeta potential (ZP). A series of *in-vitro* and *in-vivo* studies were carried out on the new formula. The produced vesicles' EE, PS, PDI, and ZP values were all good. SLNs eye drops were numerically adjusted to include carbopol, a stabilizer, lipids, and a surfactant, among other substances. ZP of -36.5 ± 0.20 mV, 80.9 ± 1.02 % EE, 205 ± 9.1 nm PS, and 0.015 PDI were all included in the data. For example, by differential scanning calorimetry (DSC) and fourier-transform infrared (FTIR), it was discovered that the crystallinity of the drug had been reduced. The *in-vitro* release study and the SLNs and carbopol-based eye drops prepared with ultrasonication method demonstrated sustained release up to 48 hours. Comparing VRN-SLNs pharmacokinetics to that of pure drug solution, researchers discovered an area under the curve (AUC) and C_{max} three times higher and a factor of five times higher, respectively (both P 0.01). By functioning as a carrier, SLNs may increase the bioavailability of VRN in the eye. The *in-vivo* studies were performed by infecting the rats with *candida* species. It was observed that VRN-loaded SLNs eye drops were more efficient in treating candidiasis. Results indicate that VRN-loaded SLNs eye drops provide a sustaining VRN topical effect and quick relief from fungal infection.

Keywords: Box-behnken design, , Hot melt extrusion, Ocular drug delivery, Pharmacokinetics, Voriconazole.

International Journal of Drug Delivery Technology (2022); DOI: 10.25258/ijddt.12.4.36

How to cite this article: Mahal RK, Al-Gawhari F. Design and Evaluation of Solid Lipid Nanoparticle Eye Drops Containing VRN for Ocular Drug Delivery. International Journal of Drug Delivery Technology. 2022;12(4):1702-1716.

Source of support: Nil.

Conflict of interest: None

INTRODUCTION

One of the many components in the creation of solid lipid nanoparticles (SLNs) is the use of surfactants to create an emulsion.[1] These nanoparticles (NPs) are attractive to the pharmaceutical and nutraceutical sectors because of their small size, vast surface area, high drug-loading capacity, and interaction of phases at the interfaces.[2] Those are the next three numbers: spray drying and high-shear mixing, ultrasonication, and high-pressure homogenization are the most common methods for manufacturing SLNs. Chemical solvents are not used in the production of SLNs, which allows for a wide range of conceivable applications. SLN also uses physiological lipids (dermal, oral, and intravenous).[3-10]

On the other hand, lipid and hydrophobic drug carriers have been shown to boost bioavailability, shield sensitive drug molecules (water, light) from environmental hazards, and control and/or target drug release. SLNs are more stable than liposomes and simpler to produce in large quantities. Different types of targeting methods may need the use of this characteristic. Colloidal drug delivery methods based on single-layer nanoparticles are biodegradable and long-lasting (SLNs).[11-14]

Treating ocular fungal infections is one of the most difficult occupations in ophthalmology. Low socioeconomic status and inadequate sanitation are all risk factors for the disease.[15] It is difficult to administer eye medications since the eye is a delicate organ with a high degree of complexity. The blinking of the eyes and the turnover of the tear film allow drugs to be absorbed in very small amounts. Before the remaining dosage can be absorbed and used to treat patients, it has to pass past the tight connections of the corneal epithelium.[16-20] Fungal infections of the eye are also more difficult to cure because they take longer to develop. Patients often decline invasive therapies like penetrating keratoplasty[21] or high doses of systemic and topical antifungals.[22,23] As a result, we must look for quicker and more efficient solutions.

Fluconazole's molecule was modified to create the second-generation triazole antifungal VRN. Even at low minimum

*Author for Correspondence: Dr.rafahkh@gmail.com

inhibitory doses, this chemical inhibits a broad variety of fungi, including *Aspergillus, Candida,* and others.[24,25] VRN may be purchased over the counter in both oral and intravenous dose forms. There are substantial adverse effects and pharmacological interactions associated with using VRN systemically. The log *p*-value of 1.8 and molecular weight of 349.3 of VRN make it an attractive option for ocular medication delivery.[26] VRN's difficulty in dissolving in aqueous solution has prevented the development of a commercial ophthalmic product. Topical therapy for individuals with fungal keratitis is injected with cyclodextrin-VRN complex lyophilized powder for intravenous injection. Consequently, patients feel unsatisfied and quit taking their medication.

NPs were made using the hot-melt extrusion (HME) technique in this investigation. Lipid-drug solutions with surfactants also have decreased viscosity and surface tension, resulting in smaller droplets and smaller NPs. Testing for antifungal activity with VRN delivered topically and *in-vitro* using the fourier-transform infrared (FTIR) spectroscopy and scanning electron microscopy (SEM) were among the methods used to evaluate the NPs. Other methods included zeta potential measurements, encapsulation efficiency, and drug content.

MATERIALS AND METHODS

Materials

VRN was given to Hetero Pvt. Ltd. as a gift (Hyderabad, Telangana, India). Also included were palmitic acid, tween 80, and tween 20, as well as acetic acid and sodium lauryl sulfate, all of which were acquired from the same source as the steric and palmitic acids (Merck KGaA, 64293 Darmstadt, Germany). Triethanolamine, carbopol, and poloxamer from Hamdard Laboratories Pvt. Ltd. also made an appearance. When it came to providing the dialysis membrane, Hi Media went above and above (Mumbai, India). Experiments were carried out using Milli-Q-plus water purification equipment (Millipore, India). All tests were carried out using analytical-grade chemicals.

SLNs Formulation

Lipids and surfactant were combined in an extruder barrel at temperatures 10–15°C over the melting point of the lipids. An extruder with two co-rotating screws extruded lipids (Compritol® 888 ATO/Precirol® ATO 5/stearic acid) before testing the VRN geometric combination (11 mm Process 11, Thermo-Fisher Scientific Karlsruhe, Germany). Through either an injection port in zone 3 or zone 4, we used a peristaltic pump to inject numerous dosages of the extrusion temperature-equivalent surfactant tween 80 (Pharmacopeia of the United States (USA)/Pluronic® F-68) into the extruder barrel. Zone 2's temperature was either 150 or 120°C, while all other zones were kept at 90°C, including the die temperature. The screw speed was either 160 or 240 rpm in all of the formulations. When hot pre-emulsion from hot-melt extrusion is passed via an insulated tube, it is homogenized in the homogenizer (Avestin Emulsiflex C5, Canada). The pre-emulsion particle size was reduced in two cycles at 85 and 1000°C bar pressure using high-pressure homogenization (HPH). All batches had the same HPH values. An SLNs was formed by cooling the emulsion to room temperature. The drug concentration (DC) and surfactant lipid concentration (SC) were both influenced by process factors such as screw speed (SS), barrel temperature (TB), and zone of liquid addition (ZLA) (ZA).[27]

Conceptualization of the Study

The performance and properties of VRN-SLNs were studied using a Box-Behnken design (BBD) screening approach. One of the most often utilized experimental designs is the BBD one. It is possible to employ the resolution three designs when just the major impacts are of interest. There are a lot of variables and fewer runs with BBD designs. The design expert stat-ease software version 12.0.3.0 was used to create 17 experiments using a BBD. To determine whether the model and the factor coefficients were statistically significant, we used multilinear regression and one-way ANOVA. Formulations for each experiment were made in threes. As dependent variables, we examined zeta potential, entrapment efficiency, and particle size (Table 1). The linear equation for the model is as follows:

$$Y=b0 + b1X1 + b2X2 + b3X3 + b4X4 + b5X5 + \ldots + bnXn$$

Factor X1, X2,..., Xn (indicating the influence of each factor ordered within the range of 1, +1) has an effect on the answer Y, and its coefficient b0 is the constant.

SLNs Solution Characteristics

Micromeritics Measurement

The resulting SLNs' mean particle size and polydispersity index (PDI) were measured using ZS Nano ZS (Malvern, USA). A dynamic light scattering method was used to quantify particle size. After diluting an SLNs sample to an appropriate concentration with water, the particle size and polydispersibility index were measured in a cuvette.[28] The zeta potential was also measured using the zetasizer nano ZS. An average of 10 runs, each with three measurements, yields the following results: Research claims that dispersion with a zeta potential larger than 20 mV is physically stable. An angle of 173°, a refractive index of 1.33, viscosity of 0.89 cP, and 25°C were utilized in the zetasizer.

Encapsulation Efficiency Measurement

SLNs were ultrafiltered and centrifuged for 20 minutes at 12,000 RPM to measure the entrapment efficiency using centrifugal filters (Amicon Ultra—0.5 with a 50 kDa cut-off from Millipore, USA). Three attempts were to determine how much free VRN could be found in the dispersion's aqueous layer. The amount of free VRN in the aqueous phase was measured using an high-performance liquid chromatography (HPLC) method with a wavelength of 256 nm.[29] Entrapment efficiency was calculated using these equations from the HPLC study.

Differential Scanning Calorimetry (DSC)

The Mettler DSC823 Mettler Ltd. in Toledo, Ohio, created differential scanning calorimetry thermograms for several types of VRN, including SLNs, bulk, and lipid mixtures. An aluminum pan with 10 mg of material was used as the last phase

Table 1: Selection of independent variables for the formulation:

Factor	*Name*	*Minimum*	*Maximum*	*Coded Low*	*Coded High*
A	Lipid Concentration (%)	5.00	10.00	-1 ↔ 5.00	+1 ↔ 10.00
B	Surfactant (%)	2.00	6.00	-1 ↔ 2.00	+1 ↔ 6.00
C	Sonication (min)	4.00	8.00	-1 ↔ 4.00	+1 ↔ 8.00

Table 2: Displays water-based solution samples with various concentrations of Carbopol 974 P.

Shear rate (r/min)	*Viscosity (cP)*		
	0.5% Carbopol 974 P	*1% Carbopol 974 P*	*2% Carbopol 974 P*
10	------	156.29 ± 12.51	1564.38 ± 25.91
20	------	135.48 ± 9.68	1294.85 ± 18.34
40	0.56 ± 0.34	122.38 ± 10.29	1057.19 ± 12.58
80	5.34 ± 2.13	106.37 ± 14.28	------
160	7.86 ± 1.28	95.68 ± 3.51	------
200	6.92 ± 0.52	83.26 ± 5.67	------
240	7.23 ± 0.16	79.64 ± 2.16	------
280	9.58 ± 0.43	------	------
320	8.94 ± 0.84	------	------
360	10.53 ± 0.95	------	------
400	12.05 ± 0.48	------	------

of the method. At a rate of 10°C per minute, the pans were heated from 30 to 300°C using an empty pan as a baseline. An inert atmosphere was maintained by pumping out 40 minutes of nitrogen gas.

Diffractometry via X-ray (XRD)

Measurements were made using X-ray diffractometers (PW 3710, Philips Ltd.). Use of the Cu–Ka radiation source allowed for 5°C scannings every minute. X-ray diffraction experiments were carried out on VRN SLNs, bulk VRN, bulk lipids, and a physical mixture of lipid and VRN.[30]

Infrared Spectroscopy using the Fourier Transform (FTIR)

Drug interactions with excipients contained in the formulation have been evaluated. Evaluated utilizing the Bruker Alpha FTIR, all three VRN samples were analyzed for their FTIR spectrum. The attenuated total reflection technique was used to get the IR spectra of the samples after a little amount of sample was placed on the sample holder. In the IR spectra, a resolution of 1 cm^{-1} was obtained in the 400–4000 cm^{-1} range.

Topical Eye Drops based on SLNs are being Developed.

Because of the compatibility with NP dispersions, gelling agents were examined for their compatibility with VRN-SLNs dispersions, feel, and spreadability (data not shown). Using carbopol 974 P as a gelling agent for topical application was shown to be effective. SLNs dispersions of carbopol 974 P were used to disperse the chemical throughout the procedure. Methyl and propyl parabens were used as a preservative. Under magnetic stirring and mixing at roughly 1000 rpm for 15 minutes, triethanolamine was gently introduced to neutralize the aforementioned dispersion. To ensure uniform dispersion and the removal of trapped air, the gel was incubated overnight. When determining the final carbopol 974 P concentration, the gel formulation's final consistency was taken into consideration.[32]

Rheological Studies to Determine the Concentration of Carbopol 974 P

Samples of water-based solutions with carbopol 974 P (w/v) concentrations of 10 to 400 r/min had their rheological properties studied at room temperature using a Brookfield rheometer (Middleboro, MA). Each sample was analyzed five times. For some reason, the Brookfield rheometer is only able to produce some of the data for the solutions of 0.5% carbopol 974 P and 2% carbopol 974 P. (maybe certain readings are outside the measuring range). Carbopol 974 P, with a viscosity of 1%, was the sole choice for further inquiry, according to Table 2.

Preparation of the VRN Water-based Eye Drops and Carbopol 974 P-based Solution

VRN water-based eye drops were prepared in line with prior findings,[33] and the results are shown in Table 3. Using VRN (0.5% by weight) and carbopol 974 P (1% by weight), a viscous solution was made by following the steps outlined below. Table 3 lists it as well (Application Number CN20151010.9). Addition of methocel F4M and overnight hydration in sterile water were used to make the VRN solution stable. Prior to ethyl addition, paraben's sodium chloride and sodium citrate adjusted the pH of the solution. Thiomersal was replaced with ethyl-paraben in the formulation for safety and stability. When the volume reached 100 , water for injection was added. The mix produced a thick solution with the excellent compatibility of carbopol 974 P and VRN. Carbopol 974 P SLNs dispersion proved to be a clear and easy-to-flow liquid. It was then transferred into 5- plastic bottles, sealed with caps, and sterilized at the manufactory laboratory of the ophthalmic center.

Table 3: The formulations of the VRN water-based eye drops and Carbopol 974 P based solution

Ingredients	*Carbopol 974 P-based solution*	*water-based eye drops*
VRN SLNs ()	10	10
Sodium chloride (mg)	125	150
Sodium citrate (mg)	50	75
Methocel F4M (mg)	150	200
Thomersal (mg)	2	4
Methylparaben (mg)	50	100
Water for injection	100	100

Table 4: Experimental Factors and Their Levels

Factors	*Significance*	*Level (-1)*	*Level (+1)*
X1	Lipid concentration (%)	5	10
X2	Surfactant (%)	2	6
X3	Sonication (min)	4	8
	Screw speed (RPM)	150	200
	The temperature of the barrel (°C)	120	150
	Adding water to a mixture	3	4

VRN Viscous Solution Rheological Investigations

Samples of VRN-SLNs viscous solution VRN 974 P-based solution were prepared, and the rheology of each sample was analyzed using the Brookfield rheometer at room temperature to measure the viscosity. A total of five evaluations were performed on each sample.[34]

Drug Administration and Sample Collection

One drop of the 1% VRN water-based eye drops (30 µL) and one drop of the carbopol 974 P-based VRN-SLNs dispersion (0.5%) were injected into the right eye's conjunctival sac as controls. Glass capillaries were used to collect 1-mL tears from the lower marginal strip 2, 5, 8, 10, 15, 20, 25, and 30 minutes after instillation. Perchloric acid (10% w/v) was used to precipitate the protein in the tear samples, and the centrifuged supernatants were stored at -40°C for HPLC analysis after they were centrifuged. After 60 minutes of drug administration, five rabbits received overdoses (100 mg/kg) of pentobarbital by intravenous injection. It was necessary to collect specimens of the eye's surface immediately after the patient had been examined, weighted, and stored at 20°C. Researchers utilized a 0.8 , 20 µg/solution of ethyl 4-aminobenzoate in methanol to homogenize conjunctiva, cornea, and sclera samples (internal standard, IS). After centrifugation, we used the supernatants, which were then resolved with 0.2 of methanol for HPLC analysis.[35] To prepare for HPLC analysis, the aqueous humor was centrifuged and then dissolved in perchloric acid at a concentration of 10%.

Quantification of Drug Release In-vitro

The paddle technique was used to perform dissolving experiments on crude VRN and commercially available micronized VRN (200 mg). Phosphate buffer (pH 7.4) containing 0.3% sodium lauryl sulfate was used to dissolve both the commercially available VRN formulation and the crude VRN (200 mg in gelatin capsules) (SDS). 1.5 of the releasing medium was withdrawn and replaced with 1.5 of new dissolving solution every 5, 10, 15, 30, 45, 60, 90, 120, 180, 240, and 300 minutes. A HPLC analysis was performed on each sample after it had been put through a 0.45-µm syringe filter. Drug release testing of SLNs formulations was carried out in dialysis bags. This is the most often referenced strategy for estimating the release of SLNs medicine. The release kinetics of NPs systems were determined using a technique similar to

Table 5: Statistical Design for the preparation of SLNs

Run	*Std*	*X1*	*X2*	*X3*	*Y1*	*Y2*	*Y3*	*PDI*
2	1	10	2	6	65.6 ± 2.15	354 ± 5.6	-22.8 ± 0.01	0.564
6	2	10	4	4	72.1 ± 0.39	486 ± 12.5	-27.3 ± 0.11	0.428
10	3	7.5	6	4	80.9 ± 1.02	403 ± 10.2	-36.5 ± 0.20	0.015
13	4	7.5	4	6	60.5 ± 2.31	330 ± 8.6	-15.6 ± 0.31	0.259
4	5	10	6	6	78.4 ± 4.01	464 ± 7.3	-24.3 ± 0.05	0.346
11	6	7.5	2	8	72.5 ± 1.22	595 ± 6.2	-28.9 ± 0.04	0.357
8	7	10	4	8	46.3 ± 3.09	546 ± 8.4	-23.7 ± 0.01	0.128
3	8	5	6	6	79.7 ± 5.16	205 ± 9.1	-26.1 ± 0.02	0.315
7	9	5	4	8	74.3 ± 2.37	482 ± 3.4	-20.6 ± 0.03	0.254
17	10	7.5	4	6	61.7 ± 0.97	320 ± 10.5	-15.9 ± 0.16	0.316
1	11	5	2	6	70.5 ± 3.15	381 ± 15.2	-19.4 ± 0.05	0.412
5	12	5	4	4	40.6 ± 2.08	326 ± 12.9	-25.1 ± 0.41	0.256
12	13	7.5	6	8	70.8 ± 3.11	298 ± 10.4	-24.5 ± 0.05	0.322
15	14	7.5	4	6	60.5 ± 2.05	320 ± 6.4	-15.9 ± 0.15	0.516
9	15	7.5	2	4	62.4 ± 1.86	294 ± 9.2	-20.6 ± 0.25	0.491
14	16	7.5	4	6	61.2 ± 5.29	320 ± 8.2	-16.1 ± 0.13	0.532
16	17	7.5	4	6	60.9 ± 1.04	320 ± 6.7	-16.3 ± 0.42	0.489

Table 6: ANOVA for the dependent variables in a quadratic model

Parameter	*Source*	*DF*	*Sum of squares*	*Mean of squares*	*F Value*	*p-Value*
Percentage of EE	Model	9	1904.97	211.66	61.80	< 0.0001
	Residual	7	23.97	3.42		
	Lack of fit	3	22.94	7.65	29.64	0.0034
	Pure error	4	1.03	0.2580		
SIZE	Model	9	1.662E+05	18470.05	64.69	< 0.0001
	Residual	7	1998.50	285.50		
	Lack of fit	3	1918.50	639.50	31.97	0.0030
	Pure error	4	80.00	20.00		
Zeta potential	Model	9	513.19	57.02	69.24	< 0.0001
	Residual	7	5.76	0.8235		
	Lack of fit	3	5.49	1.83	26.92	0.0041
	Pure error	4	0.2720	0.0680		

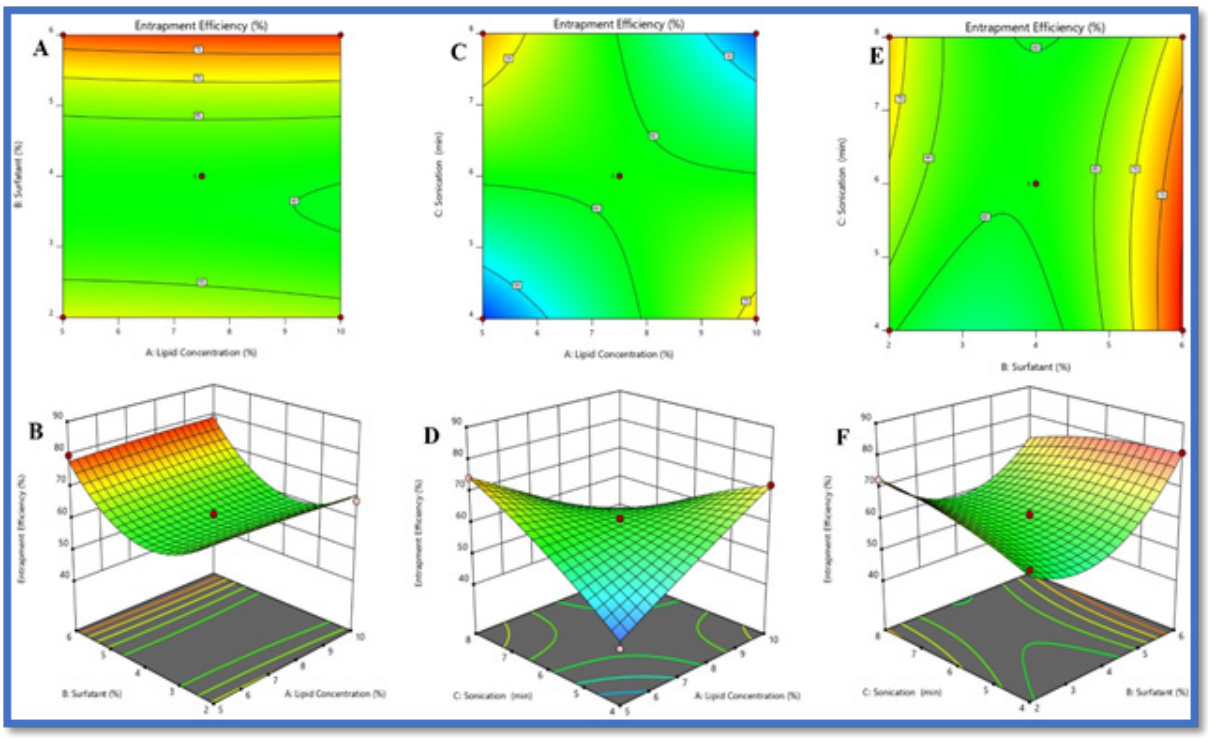

Figure 1: Contour and response surface plots of EE vs. independent variables (X1, X2, and X3.

that of Luo *et al.*[36]. The releasing media was phosphate buffer with a pH of 7.4 and an SDS content of 0.3%. Free drugs may enter the dissolving medium *via* dialysis bags with a cut-off of 10–14 kDa. After soaking for 12 hours, the bags were ready for use. The experiment was finished by adding 2 mL of dispersion to a conical flask and then sealing the bag on both ends. The conical flasks were held at 37°C and 150 rpm in a precision water bath. In order to keep the conical flask in good condition, the medium was collected and filtered on a regular basis (the same intervals used for the dissolving of crude VRN and marketed formulation). As previously mentioned, a HPLC analysis was performed to evaluate the filtrate's drug concentration. It was done in triplicate for every single one of the four raw VRN (which included the commercial version), SLNs, and VRN-SLNs eye drops formulations.

HPLC Analysis of the VRN Concentrations

Every sample was analyzed using the same HPLC parameters. An SPD-20A UV detector and Shimadzu LC-20AT separation module (Kyoto, Japan) was employed in the system (Kyoto, Japan). The HPLC separation was carried out using a Luna 5-lm C18 column (150 mm X 4.6 mm; phenomenex, torrance, CA). The column was filled to the brim using a capacity of 20 µL for each sample. In the mobile phase, acetonitrile (A) was diluted with 65% ultrapure water (B). Following multi-wavelength scanning, the flow rate and UV absorbance detector were set at 1-minute and 258 nm, respectively.

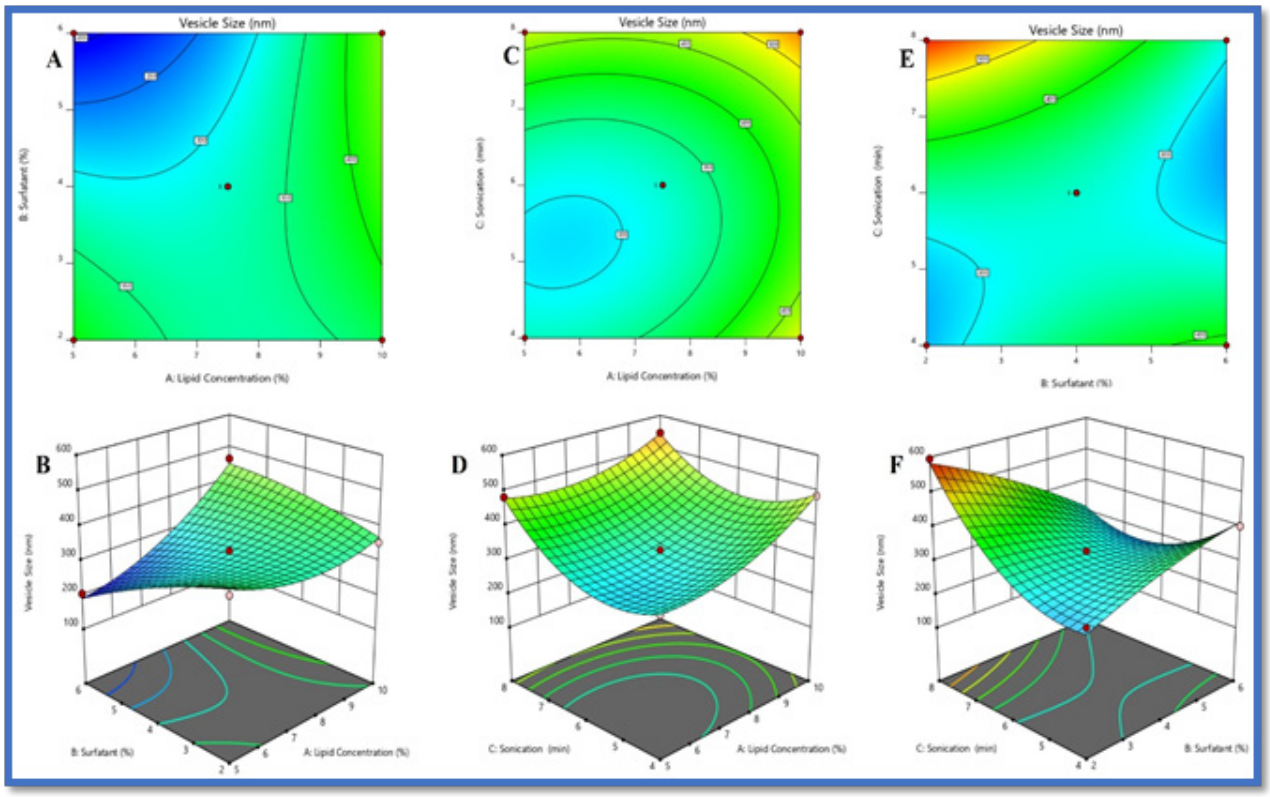

Figure 2: Vesicle size vs. independent factors in a curve plot (X1, X2, and X3).

Table 7: Skin irritation studies seen visually.

Formulation	*Irritation index*		
	24 (h)	*48 (h)*	*72 (h)*
Control	0	0	0
Plain Gel	0	0	0
VRN SLNs	0	0	0
Marketed formulation	1	3	3
VRN SLNs eye drops	0	0	0

Ocular Irritation Assessment

Slit-lamp examinations of the rabbits' eyes were performed to rule out any possible ocular abnormalities. According to the draize method, 12 rabbits were enrolled in the study. The carbopol 974 P-based solution was injected four times a day into the left eye, whereas the same quantity of saline was injected into the right eye as a control. Slit lamps were used to examine the conjunctiva, cornea, and iris for any abnormalities.[37]

Evaluation of *In-vivo* Formulations

Duration of Precorneal Retention

After injecting 100 µL of the radiolabelled solution onto the left cornea, a Toshiba GCA 602A gamma camera with a 4 mm pinhole and calibrated to detect 99mTc (MBp) radiation was used to assess the *in-vivo* pre-corneal drainage of each formulation. One to two megabits per second of activity were measured in a single 100 µL dose (MBp). A little plastic vial with a 100 µL aliquot of the fluid studied was placed near the rabbit's eye as a location marker. After instillation, the eyes were kept closed for 5 seconds to avoid solution evaporation.[38] The rabbit was put on a table with its left eye in front of the collimator aperture at a distance of 6 cm, supported by an experimenter's hand.

Using a 128 × 128 pixel grid, frames were captured for 10 minutes starting 5 seconds after installation. There were a total of three rabbits used for each of the formulations. A total of 63 frames (36 × 5 s frames followed by 12 × 10 s frames and 15 × 20 s frames) were combined to provide an overall view of label distribution. Finally, the final pictures were separated into five areas of interest (ROIs), each of which had a different focus: background, reference, pre-corneal surface, canthus, lachrymal duct.

After completing the experiment, the corneal surface was left with 10 minutes of activity remaining, which was determined as t10, AUC0–10 (the area under the curve demonstrating how much activity is remained in the pre-corneal ROI as time passes), and $t_{1/2}$ (half-life of elimination). The results are expressed using the mean standard deviation (SD). A student's t-test was used to discover statistically significant differences (p 0.05).[39]

In-vivo Pharmacokinetic Study

IACEC approved all animal care and experimentation under protocol number 14-013 at the University of Anurag India. No restrictions on food or water availability were placed on male wistar rats (250 ± 10 g, Harlan laboratories, IN, USA) with

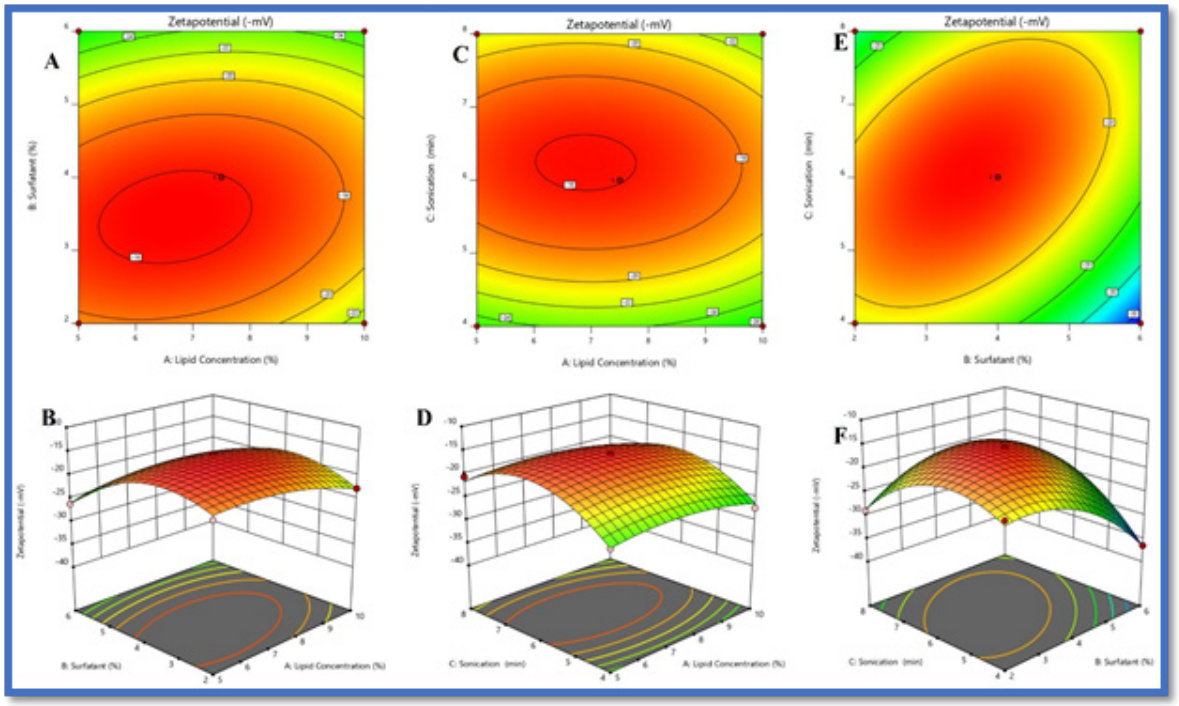

Figure 3: Contour plot of zeta potential vs independent variables (X1, X2, and X3).

Table 8: AUC0–24/MIC and Cmax/MIC ratios were used to derive optimum PK/PD indexes, other pharmacokinetic parameters

Parameters	*VRN SLNs*	*VRN SLNs eye drops*	*Marketed formulation*
Intercept	2.2638249	2.342384829	2.104540822
Slope	0.0062265	0.011498801	-0.020790547
C0 (mcg/)	183.5798	219.9808262	127.2157321
K (hr-1)	-0.0143397	-0.026481739	0.04788063
Dose (mg)	10	10	10
Dose (mcg)	1000	1000	1000
Vd ()	54.472225	45.45850733	78.6066301
Vd (L)	0.0073733	0.045458507	0.07860663
$t_{1/2}$ (hr)	-48.327239	-26.16897615	14.47349369
Clearance (l/h)	-0.0001057	-0.00120382	0.003763735
AUC $_{0\text{-}t}$ (µg.h/)	46.019949	55.12020655	31.92893304
AUC $_{1\text{-}t}$ (µg.h/)	11105	9078.75	1908.25
AUC $_{1\text{-}inft}$ (µg.h/)	-7949.9355	-9591.515069	814.5256187
AUC $_{tot}$ (µg.h/)	3201.0845	-457.6448626	2754.704552
C_{max} (µg/)	625.34	435.28	194.35
T_{max} (h)	8.024	8.0124	2.894

cannulated jugular veins for at least three days prior to the commencement of the experiment. Randomly, three groups of six rabbits each were chosen. To prepare for the experiments, rats fasted for 12 hours before receiving the formulation dosage, and food was given to them 2 hours after that. Because the oral dose of VRN was 10 mg per rabbit, 0.5 of the formulation was required for each rabbit to be given. Gavage preparations diluted the commercial micronized VRN formulation with seawater and suspended the crude drug in 0.1% SLS solution. The SLN's composition was not diluted in any way. It was pierced pre-dose at intervals of 0.5, 1, 2, 4, 6, 8, 10, and 24 hours after the medicine was given. In heparin-coated tubes, whole blood was centrifuged for 5 minutes at 12,000 rpm at 4°C to collect the plasma. Before the analysis, the plasma samples were kept in the freezer at a temperature of 80°C.

Study of Stability

An ICH Q1A (R2) stability test was performed on the new SLN formulation for 6 months. It was determined that the PB 9 design was the most stable option. In a nutshell, amber-colored

Table 9: VRN-SLNs, VRN-based eye drops, and a control (n = 3) were tested for their half-life (t1/2), residual activity after 10 minutes (t10) and area under the curve value.

Formulation	*t1/2(min)*	*t10 (%)*	*AUC0-10 (%)*
Control	2.03 ± 0.25	5.64 ± 2.38	117.54 ± 22.58
VRN SLNs	8.02 ± 5.38	16.91 ± 11.58	820.64 ± 24.69
VRN Based eye drops	8.74 ± 7.92	28.47 ± 15.62	1643.81 ± 32.57
Marketed formulation	1.56 ± 0.61	3.28 ± 1.05	98.74 ± 20.56

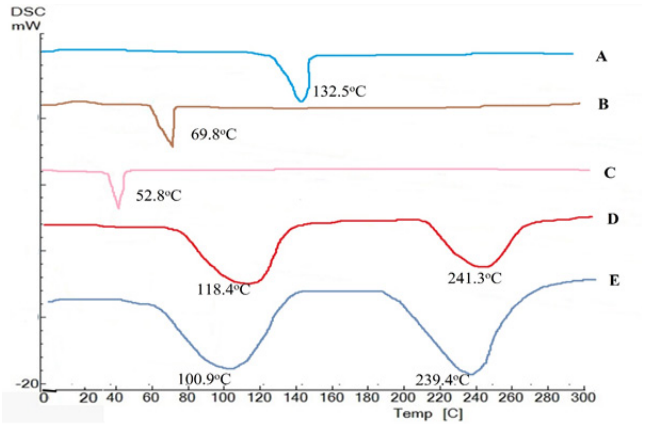

Figure 4: Analyses of the DSC spectra of the following substances: A. Pure Drug; B Stearic acid; C Poloxamer 188; D Improved formulation; and F. Carbopol-based eye solution.

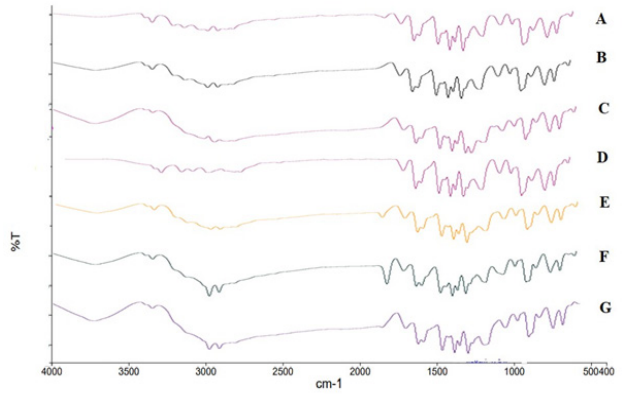

Figure 5: Voriconazole +Tristearin and Voriconazole +Palmitic Acid were analyzed using FTIR spectroscopy. Voriconazole+ Stearyl Alcohol and Voriconazole+Poloxamer188, C, D E. Voriconazole and Span 60 physical mixture G. Voriconazole SLNs Carbopol-based eye drops with an improved formulation (F3).

glass vials held samples stored at 4 and 25°C., and zeta potential (ZP), polydispersity index (PDI), entrapment efficiency (EE), and particle size were all assessed one, three, and six months into the treatment.

Statistical Analysis

The SPSS Statistics 17.0 program was used to run one-way ANOVAs where data comparisons were required (Chicago, IL). At p .05., the differences were deemed statistically significant. Unless otherwise stated, results are presented as the mean minus standard deviation.

RESULTS AND DISCUSSION

Formulation of VRN SLNs

Formulation parameters, including X1, X2, and X3, were shown to have a significant influence on the SLNs' characteristics in preliminary testing screw configuration, BT/ZA/SS, and other process parameters were shown to have a substantial influence. They used an altered screw arrangement for all SLNs formulas. The impacts of formulation and process variables were studied with the help of the BBD design approach. Four tables present data on the experimental variables and their levels, with the experimental design shown in Table 4.

Experimental Design

As a consequence of a huge number of parameters, BBD designs need a less number of tests than other screening designs. An extensive range of response variables was seen in all 17 experimental trials, which suggests that the independent factors impacted the response parameters selected. The Table 5 displays the actual and anticipated values for each of the four replies.

EE and Particle Size are Affected by Surfactant Content

Particle size and electrostatic energy were affected differently by each of the three surfactant concentrations that were examined (EE). The mean particle size increased significantly from 2 to 6% w/v of surfactant, as indicated in the experiment. Due to the decreased concentration of the surfactant, particle dispersion is more stable. When the surfactant concentration was increased from 2 to 4%, there was no significant change in the mean particle size. The results revealed that the most efficient concentration of 1% poloxamer for stabilizing SLNs dispersion was attained. The EE of several batches is shown in Figure 1. The graph clearly shows that surfactant concentration has an effect on EE. Surfactant content (2–6% w/v) was observed to rise with increasing homogenization speeds (5,000–15,000 rpm) in all batches of SLNs formulations to enhance surface coverage of nanoparticles and thereby limit drug leakage from the lipid matrix in all batches. Here is the polynomial function's equation:

Entrapment Efficiency= +60.96 -0.3375A +4.85B +0.9875C +0.9000AB -14.88AC -5.05BC -0.3675A2 +12.96B2 -2.27C2

The f-value of 61.80 indicates that this model is statistically meaningful. It is impossible that such a large noise-induced f-value would ever exist. To be deemed significant, model terms must have p-values less than 0.0500. The letters B, AC, BC, B2, and C2, include a lot of key model words. The lack of fit is clearly a major problem, as shown by the f-value of

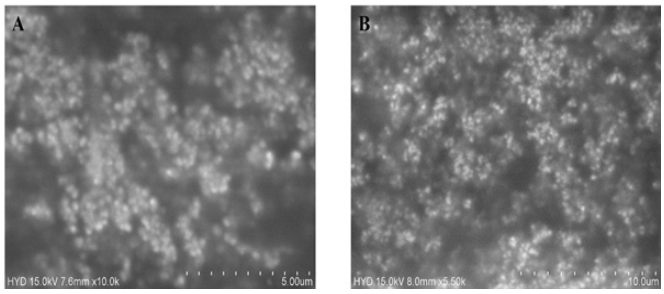

Figure 6: SEM images of A. The optimized formulation of SLNs B. Optimized Carbopol eye drops.

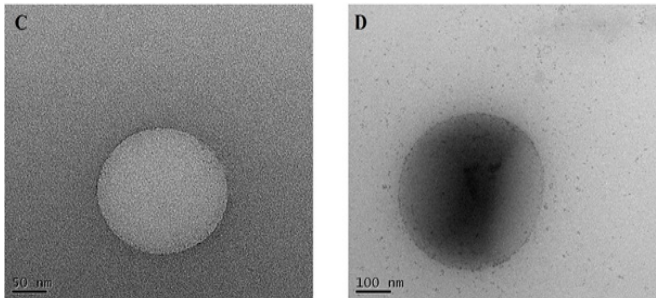

Figure 7: TEM images of A. The optimized formulation of SLNs B. Optimized Carbopol eye drops.

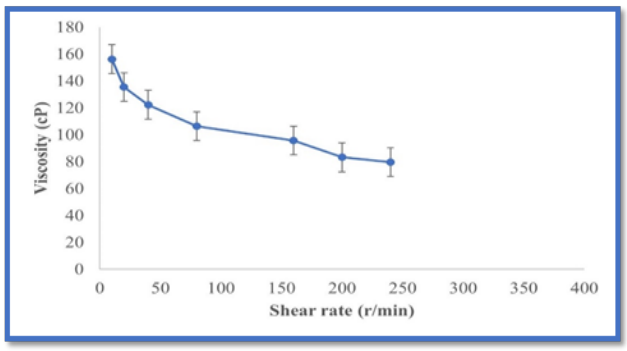

Figure 8: Solution having a viscosity of 0.5 percent VRN is viscous (Carbopol 974 P -based). The viscosities were measured at shear rates ranging from 10 to 400 r/min at room temperature. A mean standard deviation (n = 5) is shown for the data.

29.64. Noise has a 34% chance of accounting for an f-value this large due to a lack of fit. A discrepancy of less than 0.2 exists between predicted and adjusted R2s of 0.8089 and 0.9716, respectively. Adeq precision measures the signal-to-noise ratio. It is recommended that the ratio be no less than four to one. 26.605 dB is a good enough signal-to-noise ratio. This idea may help you find your way around the design environment.

Sonication Time Effects on Particle Size and Electrical Conductivity

The effect of homogenization speed on particle size and EE was studied using sonication periods ranging from 4 to 8 minutes. The sonication period was shown to have a significant impact on particle size and EE. When the sonication time is prolonged from 4 to 8 minutes, the particle size steadily decreases because particles cannot be reduced at a lower speed in less than two minutes. A decrease in particle size occurred when the sonication time period was extended due to the high shear force acting on the particles, which overpowered the intraforces working within the particles. It was interesting to see how sonication time affected entrapment efficiency in this study. EE was higher at a lower sonication time and lowered at a higher sonication duration. Because newly produced particles lack surfactant molecules, the entrapment efficiency of drugs diffuses from the lipid matrix or increases the surface area to volume ratio of small particles.

It was determined that batch F3 had the lowest particle size (403 ± 10.2 nm) and the highest entrapment effectiveness (80.9 ± 1.02%) of the three batches studied. The optimal formulation's zeta potential was determined to be -36.5 ± 0.20.

Vesicle size = +322.00 +57.00A -31.75B +51.50C +71.50AB -24.00AC -101.50BC +45.75A2 -16.75B2 +92.25C2

The model's *f*-value is 69.24, indicating statistical significance. It is impossible that such a large noise-induced *f*-value would ever exist. To be deemed significant, model terms must have *p*-values less than 0.0500. AB, BC, A2, B2, and C2 are model terms that are relevant in this situation. The *f*-value of 26.92 shows the seriousness of the lack of fit. Only 0.41 percent of the time does a very significant lack of fit *f*-value occur due to random chance. The discrepancy between the predicted R^2 of 0.8298 and the adjusted R^2 of 0.9746 is less than 0.2. Adeq precision measures the signal-to-noise ratio. It is recommended that the ratio be no less than four to one. Your signal-to-noise ratio is 29.709, according to this. This idea may help you find your way around the design environment.

Zeta potential = -15.96 -0.8625A -2.46B +1.48C +1.30AB -0.2250AC +5.08BC -1.87A2 -5.32B2 -6.35C2

We examined each response's data using Design-Expert® software (version 12.0.3.0, Stat-Ease Inc., Minneapolis, MN, USA). Coded factors for polynomial equations 1-3 are given as input by the software depending on the model that best fits the data. These equations are used to get the outcomes after the magnitude and sign of the coefficients have been taken into consideration. A lack of collaboration is shown by negative signals, but a desire to cooperate is indicated by positive signs. A statistical study using ANOVA found that the sequential model used to analyze the different factors was cubic. The Box–Cox plot of particle size and PDI suggested the inverse square root and square root response transformations to match the ANOVA assumption. The underlying models' R-squared values were compared to the adjusted ones in residual analysis and ANOVA. According to the adequacy/precision ratios, four dependent variables have an adequacy/precision ratio larger than 4.

Analysis of Variance for a Quadratic Model

Table 6.

Effect of Lipid Concentration

Impact fat content had a substantial impact on the vesicle size, PDI and zeta potential responses (Figure 2). The particle size increased significantly when the lipid content was increased. When the lipid level is large, the drug-lipid melt becomes

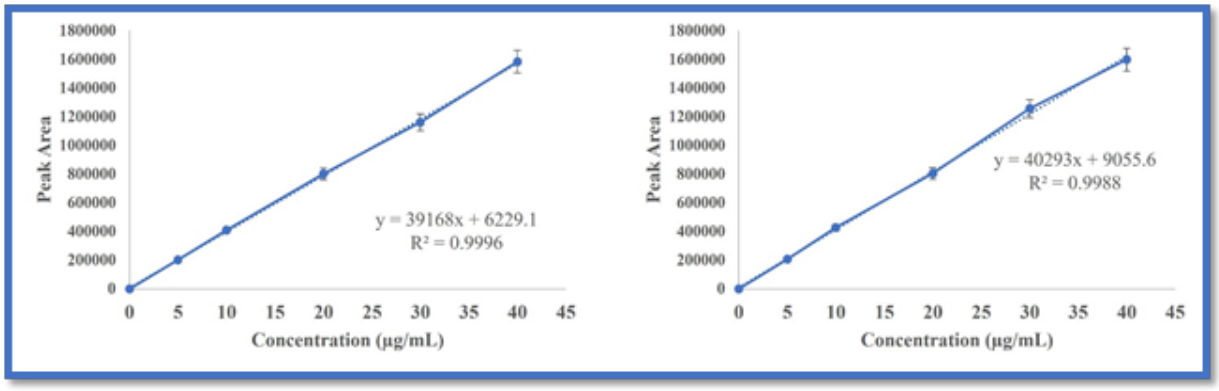

Figure 9: The VRN calibration curves for each sample. Tears, or aqueous humor, are a kind of tear fluid.

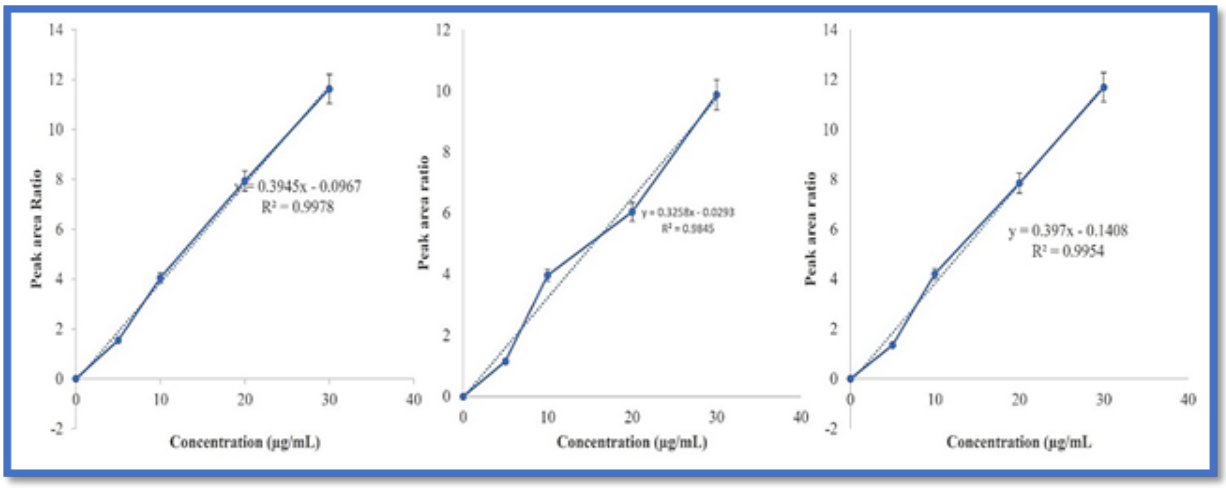

Figure 10: Different samples' VRN calibration curves are shown. (C), (D), and (E) are all the parts of the sclera.

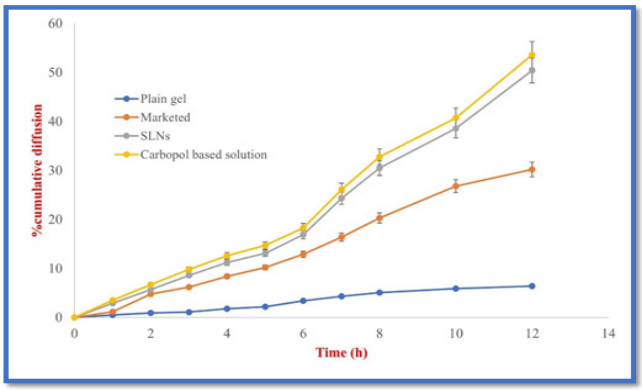

Figure 11: Compounds in eye drops, plain gel, and commercial ointment were tested for their cumulative percent cumulative diffusion through the skin membrane of human cadavers using three different formulations.

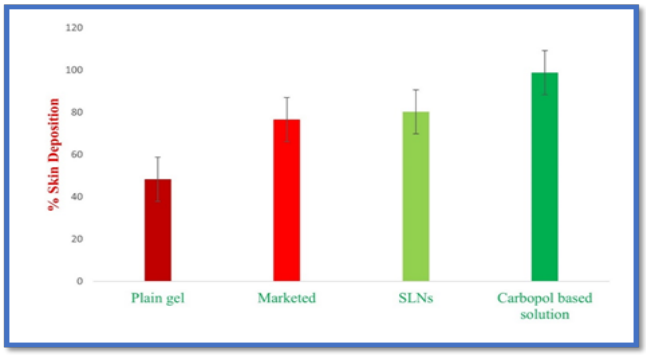

Figure 12: The percentage of VRN-SLNs eye drops, simple gel formulation, and commercialized ointment deposition in human cadaver skin membranes.

more viscous. In the early stages of emulsification, a rise in viscosity might limit homogenization, leading to larger particles and a higher PDI. As can be observed from eq. (1)'s negative coefficient, the zeta potential of the SLNs formulation decreases as the lipid content rises. The negative charge of the lipids might be to fault. As the amount of negatively charged lipids increases, so does the formulation's zeta potential. We hypothesized that EE would rise as lipid concentrations grew, and we were correct. A higher EE might be ascribed to more lipid availability for more medications' encapsulation (Figure 3).

Speed of the Screw

The PDI, zeta potential, and vesicle size were not affected by screw speed ($p > 0.05$). EE, on the other hand, felt the effects of it profoundly. Increasing the screw speed will, without a doubt, result in an increase in EE. When the screw speed is

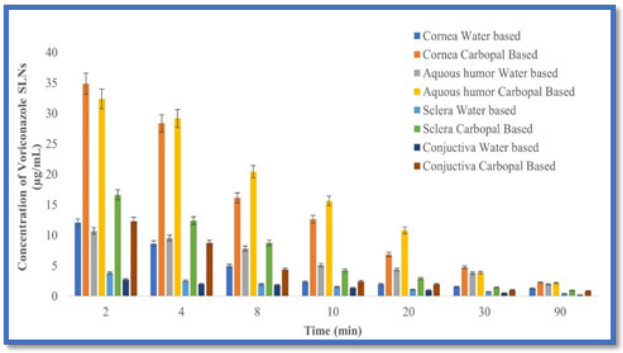

Figure 13: Virtual retinoblastoma necrosis factor (VRN-SLN) levels after the instillation of VRN-SLNs in the eye (eye drops against Carbopol 974 P-based solution).

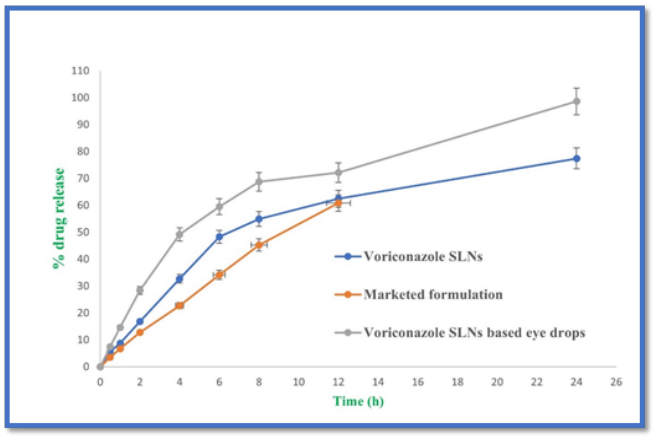

Figure 14: Dissolution characteristics of micronized VRN formulations and eye drops based on VRN SLNs generated by unique HME-HPH technique.

raised, the shear inside the barrel increases, a homogeneous emulsion may be generated by the drug, lipid, and surfactant interacting more vigorously. In this approach, the growth in EE may be explained.

Effect of Barrel Temperature

In this experiment, barrel temperature did not affect particle size. According to our findings, increasing the temperature in the barrel has an adverse effect on SLNs particle size. Because of the high temperatures in the barrel, the lipids and drugs may completely melt and become a low-viscosity liquid with no solid particles. Barrel PDI, zeta potential, and EE were not significantly different across the barrels in zones 2 and 3.

Effect of Zone of Liquid Addition

Variations in zeta potential and PDI were unaffected by the liquid addition zone. On the other hand, ZA had a substantial impact on entrapment efficiency ($p = 0.0095$). The negative ZA coefficient indicates that the EE decreases when liquid addition zones go from zone 3 to zone 4. Zone 3 and zone 4 have different melting temperatures, which might account for this. As the molten mass heats up faster in zone 3 than in zone 4, this might have an effect on the aqueous solution's ability to mix with the molten mass and produce droplets. It's possible

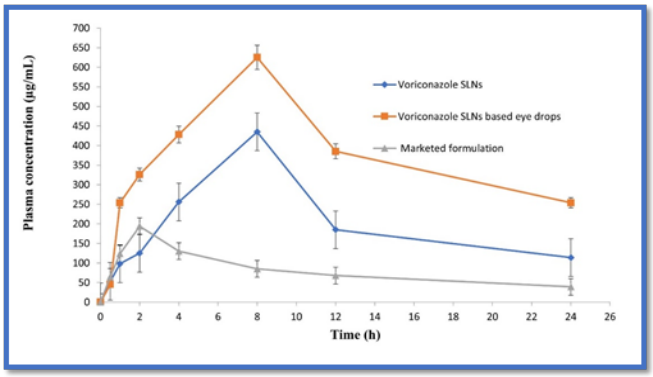

Figure 15: The average plasma concentration-time profiles of VRN after oral administration of 10 mg/kg in the rat. In addition to an HME-HPH approach, an FBT formulation, and SLN-based eye drops, three additional formulations were tested (mean SD, 4 n = 4).

to lessen EE by altering the zone of liquid addition to reduce the duration of mixing components from zone 4 to die. While it is possible to increase drug entrapment by adding surfactant solution to zone 3, it is also possible to increase the amount of shear that occurs and therefore increase the amount of lipid-drug and surfactant solution that is exposed. As the molten lipid-drug mass is lowered into zone 4, less of the lipid-drug mass is exposed to the surfactant solution. As a consequence, adding fluids to zone 4 reduces EE.

DSC Research

Excipients' interactions with drugs were tested using DSC. We employed VRN in its purest form, bulk steric acid, freeze-dried VRN and stearic acid, and drug-loaded SLNs for the DSC thermogram. The DSC thermogram is shown in Figure 4. Thermal analysis of VRN and bulk stearic acid yielded an endothermic peak at 235.7°C and 55.76°C, as seen in the DSC thermograms. After running the physical combination (1: 1) of VRN and stearic acid, no significant alteration in endothermic peak positions was found. Consequently, no chemical interactions between VRN and stearic acid were discovered to exist. Steroidal stearic acid (63.89°C) and mannitol (231.75°C) were discovered to have endothermic DSC thermogram peaks; however, the VRN peak was not seen in the thermograms. This finding suggests that VRN entrapment in SLNs occurs even when the SLNs are amorphous.

Infrared Spectroscopy Using the Fourier Transform

FTIR is used as a secondary investigation to confirm the stability of the crystalline shield. Figure 5 shows the created lyophilized VRN-loaded SLNs as well as the stacked IR spectra of the drug, lipid, polymer, and physical mix, all of which are clearly visible. According to the VRN FTIR spectrum shown below, O-H stretching happened at 3200.09–3046.04 cm^{-1}, C-N stretching at 1510.28–1451.28 cm^{-1}, and C-F stretching occurred at 1587.44–1451.28 cm^{-1} stearic acid has a 1.700 cm^{-1} IR absorption band for C=O stretching. O-stretching of Carbopol 934 was seen at 3000–2950 cm^{-1}, and the carbonyl C=O stretching band was visible at 1750–1700 cm^{-1}.

Scanning Electron Microscopy (SEM)

It was discovered that SEM showed rod-shaped particles with an even size distribution in the enhanced formulation of SLNs (Figure 6). The homogeneous and smooth surface of the lipid nanoparticle was observed. There is a good chance that these particles will be re-distributed throughout the surrounding area. For example, as shown in Figure 6 by SEM, VRN-SLNs carbopol-based eye drops feature long, thin particles with a resultant particle size of 200 nm. The surface of SLNs is smooth. These findings may be due to the fast diffusion of solvents from the low drug concentration to the lipid concentration, which may explain this observation.

Transmission Electron Microscopy (TEM) Studies

Carbopol eye drops tailored for TEM were utilized to study the form and size of optimum VRN-SLNs. Images of the VRN-loaded and optimized carbopol eye drops are displayed in Figure 7 (TEM photomicrograph). Based on zetasizer data, we found that the VRN-SLNs and carbopol eye drops formulations had non-spherical shapes and particle sizes of around 150 nm.

Rheological Studies

A similar pseudoplastic behavior was seen in the solution containing 1% carbopol 974 P, as shown in Figure 8, where the viscosity dropped as the shear rate increased.[13] When used as eye drops, the solution's viscosity was found to be just right for ease of application.

Freeze-thaw Cycle

As a result of the freezing and thawing cycles, the formulation's drug content and physical features remain constant under varying temperatures. When using VRN-SLNs-loaded carbopol eye drops, the drug concentration was found to be 96.5–100%, as opposed to 93.5–100% in the commercial formulation. The medication content and physical features of both formulations are indistinguishable, indicating that they are both stables under extreme and normal settings.

The Concentrations of VRN were Analyzed using HPLC

In the blank samples' chromatograms, there were no interference peaks. Each of these samples had a retention duration of around 4 to 7 minutes, respectively. Figure 9 shows the calibration curves for VRN-SLNs in different samples (Figure 10). The concentrations of VRN-SLNs in tear samples ranged from 0.412–40.395 µg with a straight standard curve. Quantities of 0.13–37.500 µg were found in aqueous humor samples of this compound as well. There was a concentration range of 0.500–37.500 µg in the conventional conjunctiva, cornea, and sclera curves.

Pharmacokinetic and Pharmacodynamic Experiments in Animals

When determining the cumulative percentage diffusion of VRN-SLNs eye drop formulation via human skin, diffusion research was carried out. All formulations released little amounts of medication throughout the first hour of the study, but penetration remained within the required range by the conclusion (not more than 6%). The polymeric matrix of gelling agents may have had a role in this outcome. For example, a statistical investigation found that after 12 hours, the permeability of the VRN-SLNs solution formulation was much lower than the permeability of the basic gel and commercial formulation. According to a study of the literature, the most effective topical drug delivery systems should have little penetration or diffusion through the epidermal membrane in order to get the maximal concentration of medication at their target area. This finding is consistent with this conclusion (epidermis and dermis). As a result, the drug's systemic adverse effects will be reduced since they will no longer be accessible. Figure 11 shows the results of a skin deposition study on human cadaver skin, with plain gel, commercial formulation, and VRN-SLNs eye solution all shown. After a 12 hours treatment, the VRN-SLNs-loaded carbopol gel showed significantly higher drug concentrations ($p \geq 0.05$) in the skin compared to the plain gel and commercial formulations. When utilizing this gel, just 8.68% of the whole medicine was discovered in the receptor compartment. However, compared to ordinary gel (about 43.06% unabsorbed), the marketed formulation (approximately 21.85% unabsorbed on the skin) was much less effective. This might be because the new formulation has a larger concentration of the active ingredient. Drug concentrations in the skin are necessary for dermatological treatment to be successful. When NPs were dispersed on the skin, more medicine remained on top of the epidermis, and less reached the receptors. Colloidal particle drug carriers like SLNs, for example, seem to be capable of delivering medication to the skin. Colloidal carriers that have a submicron particle size are able to penetrate the skin because of their lipoidal shape, making it easier to target the medication to specific areas.

Concentrations of VRN in Tears

Figure 12 shows the amounts of VRN in tear fluids after a single injection of 30l of carbopol 974 P-based solution or water-based eye drops. Compared to 0.5% VRN eye drops, carbopol 974 P-based solution instillation significantly increased the tear fluid VRN content (p.01) and prolonged the medicine residence time from 10 to 30 minutes.

VRN Levels in the Eye's Tissues

Figure 13 shows the mean VRN levels over time in each ocular tissue after a single injection of 0.5% viscous solution or water-based eye drops. VRN-SLNs concentrations in the ocular tissues (e.g., cornea, conjunctiva, and sclera) were raised by carbopol 974 P-based solution compared to the eye drops. Carbopol 974 P-based solution was instilled 15 minutes after treatment, however, enhanced VRN-SLNs concentrations in the cornea and conjunctiva persisted for 30 minutes and in the sclera for an additional 90 minutes, as seen in the figure.

Inflammation of the Eyes is the Subject of Research.

The corneas, conjunctivas, and iris of the animals were examined one week after the medicine was administered, and no aberrant clinical symptoms or damage were seen. The carbopol 974 P-based VRN-SLNs solution did not irritate the

eyes, as determined by the Draize criterion, with an average score of zero.

Skin Irritation Test

An ideal delivery method should be able to eliminate the erythematic episodes that are a key drawback of VRN treatment, which severely restricts its usefulness and acceptance by patients. Table 7 shows the findings of skin irritation experiments based on eye observation. Patient and skin tolerability are both improved thanks to the decreased degree of irritation caused by the VRN-SLNs-based gel as compared to the currently available formulation. An undamaged rabbit skin test showed no scaling after using the gels and their equivalent placebos in comparison to the commercially available formulation.

Quantification of Drug Release *In-vitro*

The reduced irritation generated by the VRN-SLNs-based gel as compared to the presently available formulation, improves both patient and skin tolerability. The commercially available formulation showed no scaling on rabbit skin after using the gel and its corresponding placebos. To get the medication into release media, the SLNs released their drug into the dialysis bag. The dialysis membrane then diffused the drug out into the release medium. Medication release studies reveal that VRN-SLNs formulation (F3) released 97% of its drug after 24 hours, commercially available micronized VRN formulation (F1) released 60%, and ocular drops (F3) released an impressive 98% of its drug after 24 hours. VRNs may have a faster dissolving rate because of their smaller particle size (from a few microns for the crude VRN and marketed micronized formulation to a few nanometers for SLNs). An increase in the surface area of medication will lead to a faster dissolution rate, according to the Nernst-Noyes-Whitney equation (Figure 14).

***In-vivo* Pharmacokinetic Study**

The Pharmacokinetic parameters of VRN from both formulations were found to be different. VRN clearance was decreased by half when compared to VFEND®; AUC0–24 was raised 2.5-fold, and the medication volume of distribution was lowered. AUC0–24/MIC and C_{max}/MIC ratios were used to derive optimum PK/PD indexes, which are reported in Table 8, as well as other pharmacokinetic parameters. After 10 mg/kg IV treatment of two distinct VRN formulations to Balb/c mice, the following pharmacokinetic and pharmacodynamic characteristics were determined:

Figure 15 shows the blood concentration profiles that were obtained after VFEND® and VRN-SLNs injections were administered to Balb/c mice. At each given time point, VRN levels were higher than VFEND® when administered through SLNs. In the first hour after administration, VRN metabolism is reduced by 30% when encapsulated in eye drops, limiting the production of the inactive metabolite (VRN). There were 55.12020655 and 46.019949 mg/ of VRN in the blood at the beginning of therapy for both VFEND® and VRN-SLNs

Figure 15 depicts the pharmacokinetic and biodistribution patterns of VRN in three different formulations. A 10 mg/kg AUC0–24 of VRN administered from SLNs and VFEND® formulations is shown in the intravenous AUC0–24 (A). Metabolite concentrations (VRN SLNs-based eye drops) were measured one hour after intravenous injections of the formulations. Each group has a mean SD of twelve (n = 12 animals). Tissue distribution of the liposomal formulation administered intravenously (IV) 4 hours after the VFEND® (sulfobutyl ether-beta-cyclodextrin sodium)-complexed VRN (black bars). Bar graphs depict the n-sample std. dev. (*indicates p.05).

Duration of Pre-corneal Retention

Table 9 shows how pre-corneal drainage properties change as a function of time (10 minutes dynamic imagining). Pre-corneal residence time (AUC010 min values) were significantly longer in formulations containing carbopol (F3) or lipid (F3) alone than in an ophthalmic solution (control). By adding eye drops with carbopol-based ingredients to the control, we saw an improvement of 2.6%. When using VRN-based eye drops, clearance of formulations was delayed from the precorneal area by 4.0- to 18.42-fold than when using ophthalmic solution alone. It was shown that SLNs had a residual activity of 78.66 percent after 10 minutes, which was 6.3 times more than that of eye drops ($p \leq 0.01$). To put it another way, the presence or absence of 1% carbopol had no effect on the AUC0-10 minutes and $t_{1/2}$ values in the formulation's mean pre-corneal residence time. Pre-corneal retention is better with F3 than with polymer-only systems, according to these results (1% carbopol-based eye drops and VRN-SLNs).

Stability Study

This study's findings were statistically insignificant based on the methods used to measure particle size, zeta potential, and particle distribution index ($p \geq 0.05$). After six months of storage at 25°C, the particle size grew significantly. However, the size of the particles did not change. After six months, storing voriconazole SLNs at 25 and 4°C reduced their entrapment efficiency. However, the modifications were minor. The physical stability of voriconazole SLNs was shown over the six-month study period while they were kept at 4 and 25°C.

CONCLUSION

Topical formulations requiring better skin hydration and medication penetration may benefit greatly from SLNs, which are a very effective, non-irritant carrier. By way of example, the hot melt emulsification technique was used to make stearic acid-based SLN dispersions, which were then successfully incorporated into carbopol polymeric gel, enabling easy topical administration of voriconazole SLNs-based carbopol eye drops. Because it contains voriconazole SLNs, the topical gel is occlusive and releases the medication more slowly than standard gel. The enhanced stability and encapsulation of voriconazole in the SLNs developed may improve skin disease treatment and patient compliance. It was found that SLN was able to function as a local and site-specific method of medication delivery.

REFERENCES

1. zur Mühlen A, Schwarz C, Mehnert W. Solid lipid nanoparticles (SLN) for controlled drug delivery–drug release and release mechanism. European journal of pharmaceutics and biopharmaceutics. 1998 Mar 1;45(2):149-55.
2. Cavalli R, Caputo O, Gasco MR. Solid lipospheres of doxorubicin and idarubicin. International journal of pharmaceutics. 1993 Jan 1;89(1):R9-12.
3. Freitas C, Müller RH. Spray-drying of solid lipid nanoparticles (SLNTM). European Journal of Pharmaceutics and Biopharmaceutics. 1998 Sep 1;46(2):145-51.
4. Domb AJ. Liposphere parenteral delivery system. InProc Intl Symp Control Rel Bioact Mater 1993 (Vol. 20, pp. 346-347).
5. Zur Mühlen A. Feste Lipid Nanopartikel mit prolongierter Wirkstoffliberation: Herstellung, Langzeitstabilität, Charakterisierung, Freisetzungsverhalten und-Mechanismen (Doctoral dissertation, Verlag nicht ermittelbar).
6. Eldem T, Speiser P, Hincal A. Optimization of spray-dried and-congealed lipid micropellets and characterization of their surface morphology by scanning electron microscopy. Pharmaceutical research. 1991 Jan;8(1):47-54.
7. Müller RH, Maaβen S, Weyhers H, Specht F, Lucks JS. Cytotoxicity of magnetite-loaded polylactide, polylactide/glycolide particles and solid lipid nanoparticles. International Journal of Pharmaceutics. 1996 Jul 12;138(1):85-94.
8. Mohammed IA, Ghareeb MM. Investigation of Solubility Enhancement Approaches of Ticagrelor. Iraqi Journal of Pharmaceutical Sciences (P-ISSN: 1683-3597, E-ISSN: 2521-3512). 2018 Jun 3;27(1):8-19.
9. Mehnert W, Mäder K. Solid lipid nanoparticles: production, characterization and applications. Adv Drug Deliver Rev. 2001, 47 (2–3): 165-196.
10. Olbrich C, Kayser O, Müller RH. Lipase degradation of Dynasan 114 and 116 solid lipid nanoparticles (SLN)—effect of surfactants, storage time and crystallinity. International journal of pharmaceutics. 2002 Apr 26;237(1-2):119-28.
11. Muller RH, Maader K, Gohla S. Solid lipid nanoparticle (SLN) for controlled drug delivery-review of the state of the art. Eur J Pharm Biopharm. 2000, 50: 161-177.
12. Muller RH, Runge SA. Solid lipid nanoparticles (SLN) for controlled drug delivery. Submicron Emulsions in Drug Targeting and Delivery. Edited by: Benita S. 1998, 219-234. Amsterdam: Harwood Academic Publishers
13. Jenning V, Gysler A, Schafer-Korting M, Gohla S. Vitamin A loaded solid lipid nanoparticles for topical use: occlusive properties and drug targeting to the upper skin. Eur J Pharm Biopharm. 2000, 49 (3): 211-218.
14. Deibel JP, Cowling K. Ocular inflammation and infection. Emerg Med Clin North Am. (2013). 31:387–97.
15. Thomas PA, Kaliamurthy J. Mycotic keratitis: epidemiology, diagnosis and management. Clinical Microbiology and Infection. 2013 Mar 1;19(3):210-20.
16. Gaudana R, Ananthula HK, Parenky A, Mitra AK. Ocular drug delivery. The AAPS journal. 2010 Sep;12(3):348-60.
17. de Sá FA, Taveira SF, Gelfuso GM, Lima EM, Gratieri T. Liposomal voriconazole (VOR) formulation for improved ocular delivery. Colloids and Surfaces B: Biointerfaces. 2015 Sep 1;133:331-8.
18. Liu S, Jones LW, Gu FX. Nanotechnology and nanomaterials in ophthalmic drug delivery. InNano-Biomaterials for ophthalmic drug delivery 2016 (pp. 83-109). Springer, Cham.
19. Pathak Y, Sutariya V, Hirani AA, editors. Nano-biomaterials for ophthalmic drug delivery. Basel, Switzerland:: Springer; 2016 Nov 12.
20. Alruwaili NK, Imam SS, Alotaibi NH, Alhakamy NA, Alharbi KS, Alshehri S, Afzal M, Alenezi SK, Bukhari SN. Formulation of chitosan polymeric vesicles of ciprofloxacin for ocular delivery: box-behnken optimization, in vitro characterization, HET-CAM irritation, and antimicrobial assessment. AAPS PharmSciTech. 2020 Jul;21(5):1-6.
21. Khater MM, Shehab NS, El-Badry AS. Comparison of mycotic keratitis with nonmycotic keratitis: an epidemiological study. Journal of ophthalmology. 2014 Dec 7;2014.
22. Mandell KJ, Colby KA. Penetrating keratoplasty for invasive fungal keratitis resulting from a thorn injury involving Phomopsis species. Cornea. 2009 Dec 1;28(10):1167-9.
23. Tilak R, Singh A, Maurya OP, Chandra A, Tilak V, Gulati AK. Mycotic keratitis in India: a five-year retrospective study. The Journal of Infection in Developing Countries. 2010 Mar 23;4(03):171-4.
24. Manzano-Gayosso P, Hernández-Hernández F, Méndez-Tovar LJ, Gómez-Leal A. Mycotic keratitis in an eye care hospital in Mexico City. Revista iberoamericana de micologia. 2010 Mar 24;27(2):57-61.
25. Marangon FB, Miller D, Giaconi JA, Alfonso EC. (2004). In vitro investigation of voriconazole susceptibility for keratitis and endophthalmitis fungal pathogens. Am J Ophthalmol 137:820–5.
26. Theuretzbacher U, Ihle F, Derendorf H. (2006). Pharmacokinetic/pharmacodynamic profile of voriconazole. Clin Pharmacokinet 45:649–63.
27. Veloso DF, Benedetti NI, Ávila RI, Bastos TS, Silva TC, Silva MR, Batista AC, Valadares MC, Lima EM. Intravenous delivery of a liposomal formulation of voriconazole improves drug pharmacokinetics, tissue distribution, and enhances antifungal activity. Drug delivery. 2018 Jan 1;25(1):1585-94
28. Hussein AA. Ex-vivo Ex-Vivo Absorption Study of a Novel Dabigatran Etexilate Loaded Nanostructured Lipid Carrier Using Non-Everted Intestinal Sac Model. Iraqi Journal of Pharmaceutical Sciences (IJPS). 2019 Dec 22;28(2):37-45.
29. Das S, Ng WK, Kanaujia P, Kim S, Tan RB. Formulation design, preparation and physicochemical characterizations of solid lipid nanoparticles containing a hydrophobic drug: effects of process variables. Colloids and surfaces b: biointerfaces. 2011 Nov 1;88(1):483-9.
30. Shah RM, Malherbe F, Eldridge D, Palombo EA, Harding IH. Physicochemical characterization of solid lipid nanoparticles (SLNs) prepared by a novel microemulsion technique. Journal of colloid and interface science. 2014 Aug 15;428:286-94.
31. Bhalekar M, Upadhaya P, Madgulkar A. Formulation and characterization of solid lipid nanoparticles for an anti-retroviral drug darunavir. Applied Nanoscience. 2017 Feb;7(1):47-57.
32. Gaffney JS, Marley NA, Jones DE. Fourier transform infrared (FTIR) spectroscopy. Characterization of Materials. 2002 Oct 15:1-33.
33. Jenning V, Gohla SH. Encapsulation of retinoids in solid lipid nanoparticles (SLN). Journal of microencapsulation. 2001 Jan 1;18(2):149-58.
34. Sun G, Lin X, Zhong H, Yang Y, Qiu X, Ye C, Wu K, Yu M. Pharmacokinetics of pirfenidone after topical administration in rabbit eye. Molecular vision. 2011;17:2191.

35. Nief R, Hussein A. Preparation and evaluation of meloxicam microsponges: As transdermal delivery system. LAP LAMBERT Academic Publishing; 2015.
36. Kumar S, Himmelstein KJ. Modification of in situ gelling behavior of carbopol solutions by hydroxypropyl methylcellulose. Journal of pharmaceutical sciences. 1995 Mar 1;84(3):344-8.
37. Luo Y, Chen D, Ren L, Zhao X, Qin J. Solid lipid nanoparticles for enhancing vinpocetine's oral bioavailability. Journal of controlled release. 2006 Aug 10;114(1):53-9.
38. Alkawak RS, Rajab NA. Lornoxicam-Loaded Cubosomes:-Preparation and In vitro Characterization. Iraqi Journal of Pharmaceutical Sciences (P-ISSN 1683-3597 E-ISSN 2521-3512). 2022 Jun 17;31(1):144-53.
39. Tashakori-Sabzevar F, Mohajeri SA. Development of ocular drug delivery systems using molecularly imprinted soft contact lenses. Drug development and industrial pharmacy. 2015 May 4;41(5):703-13.
40. Jia Z, Lin P, Xiang Y, Wang X, Wang J, Zhang X, Zhang Q. A novel nanomatrix system consisted of colloidal silica and pH-sensitive polymethylacrylate improves the oral bioavailability of fenofibrate. European journal of pharmaceutics and biopharmaceutics. 2011 Sep 1;79(1):126-34.
41. Alwan RM, Rajab NA. Nanosuspensions of Selexipag: Formulation, Characterization, and in vitro Evaluation. Iraqi Journal of Pharmaceutical Sciences (P-ISSN: 1683-3597, E-ISSN: 2521-3512). 2021 Jun 15;30(1):144-53.